

1 **In-depth characterization of phosphate intercalated MgAl Layered double hydroxides and study**  
2 **of the PO<sub>4</sub> release properties**

3 Alexandra Jourdain<sup>†</sup>, Christine Taviot-Gueho<sup>†</sup>, Ulla Gro Nielsen<sup>‡</sup>, Vanessa Prévot<sup>†\*</sup>, Claude Forano<sup>†\*</sup>

4 <sup>†</sup>Université Clermont Auvergne, CNRS, INP Clermont, Institut de Chimie de Clermont- Ferrand, F-  
5 63000 Clermont-Ferrand, France

6 <sup>‡</sup>Department of Physics, Chemistry and Pharmacy, University of Southern Denmark, Campusvej 55,  
7 5230 Odense M, Denmark

8

9 **Supporting Information**

10 **Experimental section**

11 *Mg<sub>2</sub>AlCl-LDH Synthesis*

12 A 3.0 L solution of the metal salts with a total metal concentration of 2.5 M and the Mg/Al molar ratio  
13 equal to 2 was added by a peristaltic pump at a rate of 10 mL/min to 4 L deionized water in a large  
14 scale reactor (15 L). A nitrogen (N<sub>2</sub>) atmosphere was used to minimize the carbonate contamination.  
15 The pH of the synthesis solution was kept constant (pH=10) by the simultaneous addition of a 5 M  
16 NaOH solution using a peristaltic pump that is monitored by a pHmeter connected to a pH electrode  
17 immersed in the reactor. Subsequently, the suspension was aged for 78 h at room temperature, then  
18 collected by centrifugation before the solid product was washed thrice with deionized water, dried at  
19 40 °C and finally grinded to obtain a fine powder. 546 g of LDH were obtained in a homogenous one  
20 batch corresponding to a yield of 87 %.

21 *Protocol of mineralization of solid samples for ICP-OES analysis*

22 LDH matrices dosed by ICP-OES were first mineralized. 50.0 mg of powdered LDH were introduced  
23 into a hermetically sealed Teflon microwave reactor (MW5000 Anton Paar) in 2 mL HCl and 6 mL  
24 HNO<sub>3</sub>. The reactors were placed in an Anton-Paar microwave oven and heated (10°C/min ramp) at  
25 230°C for 30 min. The acidic solutions were then recovered and diluted in a 50 mL volumetric flask  
26 with deionized water. The solutions as well as some supernatants were dosed by ICP-OES (standard  
27 range from 0.01 mg/L to 50 mg/L), and in particular, the concentration of Mg, Al, P, and K in the  
28 supernatant were determined by ICP-OES.

### 29 *Soil juice extraction*

30 The procedure for extracting soil juice was inspired by the procedure for determining soil pH. The soil  
31 sample was dried at 40°C in an oven for 24 hours, then ground to obtain grains with a diameter of less  
32 than 2 mm. For the production of one liter of soil solution, 150 g of dry soil (V<sub>soil</sub> ~170mL) were  
33 introduced into a 1L flask and a volume of deionized water (V<sub>H<sub>2</sub>O</sub>) equal to five times V<sub>soil</sub> were  
34 added. The closed flask was stirred for one hour on an orbital shaker, then the mixture was left to stand  
35 for an hour. The soil juice was then recovered by vacuum filtration (Büchner) after homogenization of  
36 the mixture (pH = 7.1). The elements of interest present in the soil juice were dosed to obtain a "blank"  
37 which was subtracted to calculate the release rate.

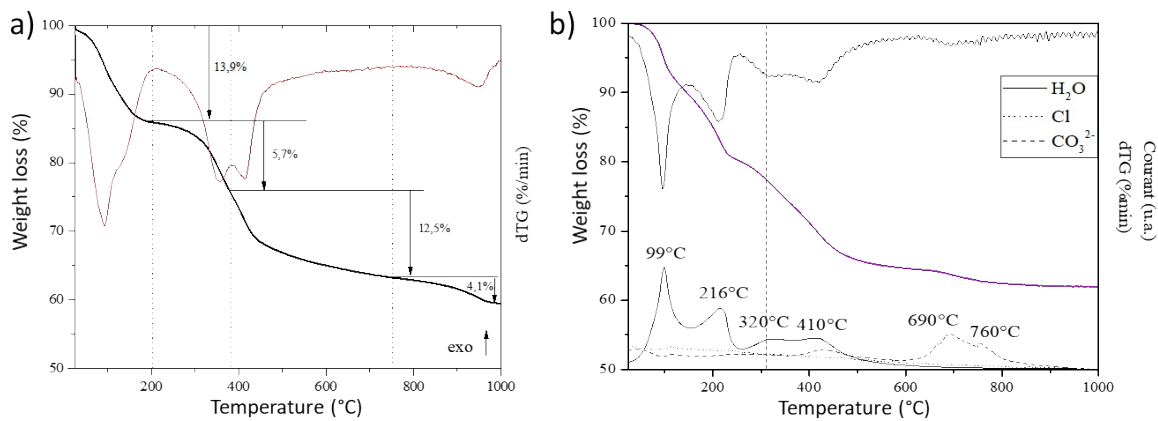
### 38 *Pair Distribution function analysis*

39 The simulated PDF for Mg<sub>R</sub>Al hydroxide layers were calculated using PDFgui software<sup>1</sup>. Powder  
40 samples ground with a mortar were placed in glass capillaries of 0.7 mm diameter. An empty capillary  
41 of the same type was measured in the same way for background subtraction. Data were recorded over  
42 the 1-145° 2θ range, which corresponds to an accessible maximum value for the scattering vector Q  
43 max of 21.4 Å<sup>-1</sup>. Data merging, background subtraction, and Kα<sub>2</sub> stripping were done using  
44 HighScore Plus software provided by PANalytical Corporation. It was also used to generate a corrected  
45 and normalized total scattering structure functions S(Q) and considering the bulk chemical

46 compositions given in Table 1. Finally, the PDF or  $G(r)$  were calculated from the Fourier transforms  
47 of  $S(Q)$  truncated at  $21 \text{ \AA}^{-1}$ . The comparison with  $\text{Mg}_2\text{AlCO}_3$  (from a previous unpublished study)  
48 and  $\text{Mg}_2\text{AlCl}$  reference samples clearly shows that phosphate intercalation leads to significant changes  
49 on the PDF. All the contributions of all pairs of atoms add up in the PDF and the integrated intensity  
50 of PDF peaks depends both on the number of atoms pairs occurring at the respective distances and on  
51 the X-ray scattering power of the atoms involved in these pairs. Here, the distance range examined is  
52 limited to the interlayer distance, thereby the peaks observed are mainly from distances of the  
53 hydroxide layer plus one interlayer. In the case of LDH, a major contribution is expected from the  
54 hydroxide layer on PDF peaks while the contribution of the interlayer species, which have weaker  
55 scattering and are subject to significant static and dynamic disorders (base of the peaks). Thus, the six  
56 main peaks labelled P1 to P6 are often considered as dominated by the contributions of M-OH and M-  
57 M pairs corresponding to the successive coordination shells around cations as shown in Figure S2B.  
58 The contributions of interlayer species can modify the intensity of M-OH pairs as shown here  
59 according to their scattering power.

60 <sup>1</sup> C L Farrow, P Juhas, J W Liu, D Bryndin, E S Božin, J Bloch, Th Proffen and S J L Billinge,  
61 PDFfit2 and PDFgui: computer programs for studying nanostructure in crystals. *J. Phys.: Condens.*  
62 *Matter* 19 335219. DOI 10.1088/0953-8984/19/33/335219

63 Figures

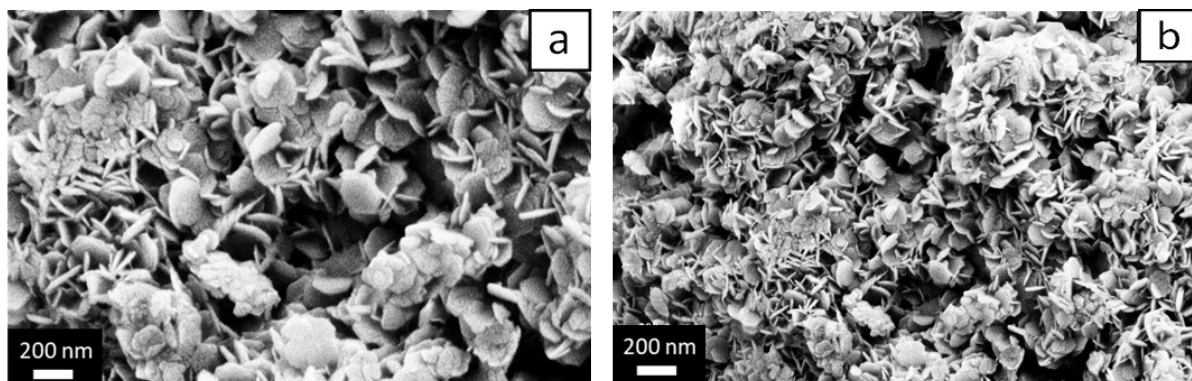


64

65 Figure S1. TGA and DTG analyses of Mg<sub>2</sub>AlCl a) and Mg<sub>2</sub>AlP b) in the case of the latter, the

66 analysis was coupled with mass spectroscopy

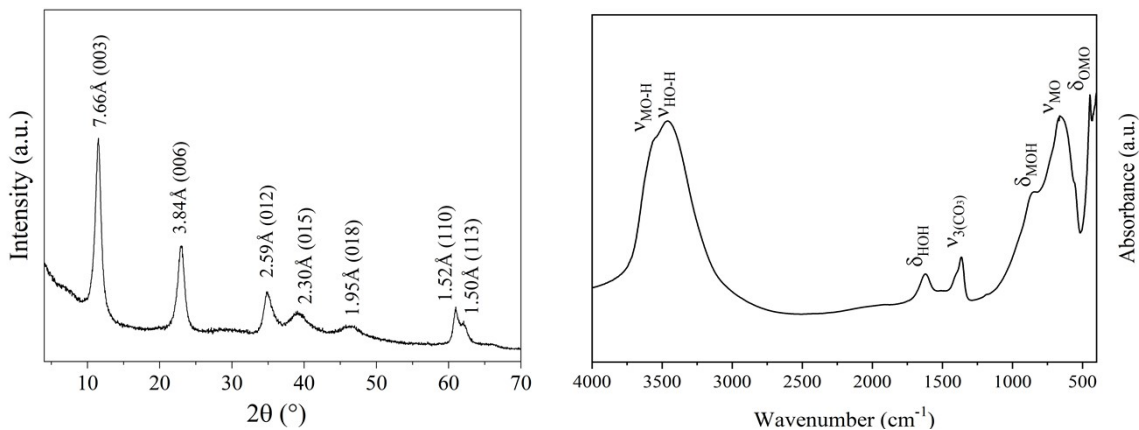
67



68

69 Figure S2. SEM images of Mg<sub>2</sub>AlCl a) and Mg<sub>2</sub>AlP b)

70

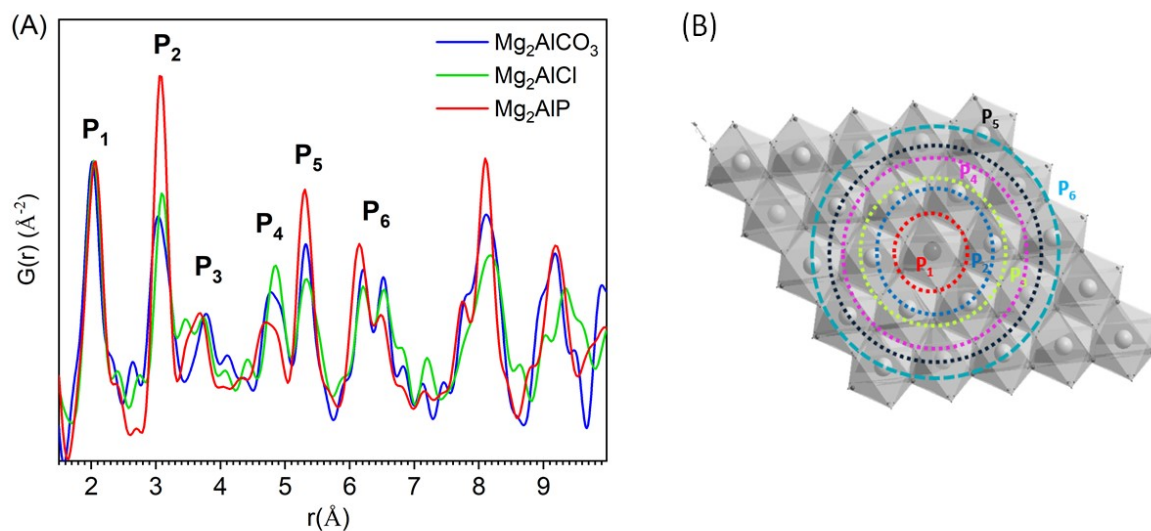


71

72 Figure S3. XRD pattern of  $\text{Mg}_2\text{AlCl}$  (left), FTIR spectrum of  $\text{Mg}_2\text{AlCl}$  (right)

73

74



75

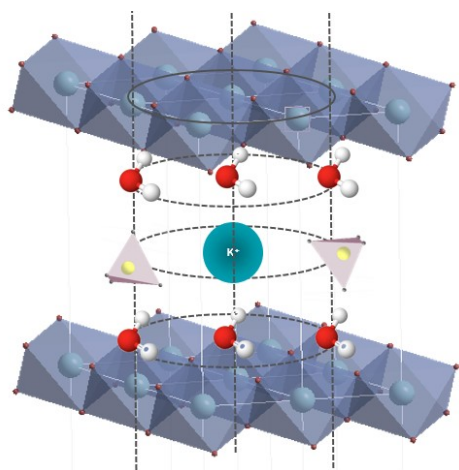
76 Figure S4. Experimental pair distribution function (PDF) also known as  $G(r)$  for  $r < 10 \text{ \AA}$  for:

77  $\text{Mg}_2\text{AlCO}_3$  (blue line),  $\text{Mg}_2\text{AlCl}$  (green line),  $\text{Mg}_2\text{AlP}$  (red line) (A). Representation of the edge-

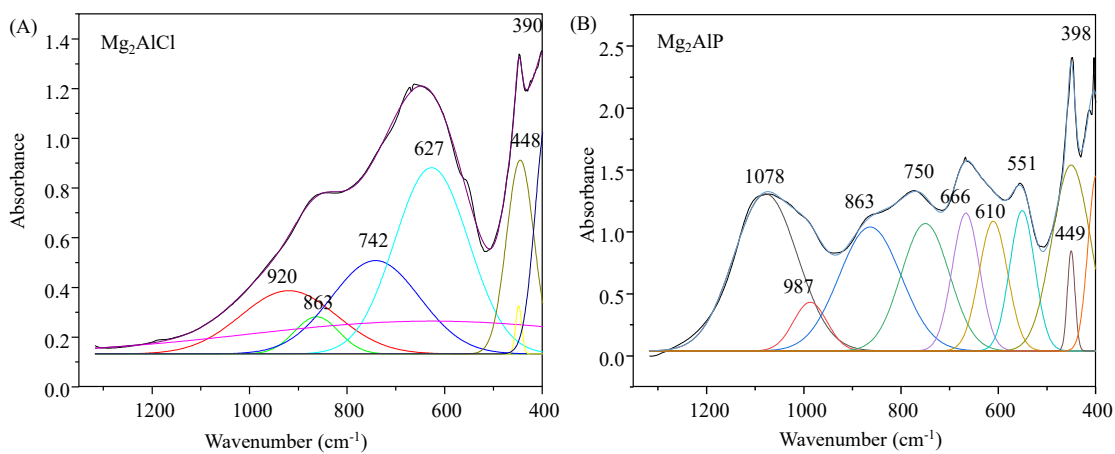
78 sharing octahedral layer where the contributions P1 to P6 are materialized (see text) (B).

79

80



81 Figure S5. Schematic representation of the arrangement of interlayer species in sample  $Mg_2AlP$  on  
 82 P2 coordination shell.

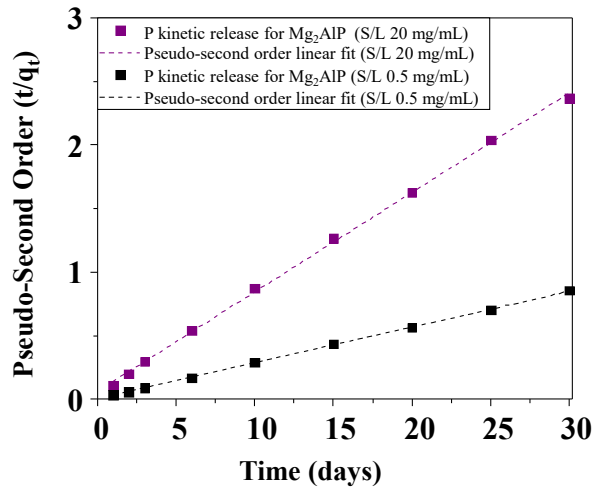


83  
 84 Figure S6. Deconvolution of FTIR spectra in the low energy domain of (A)  $Mg_2AlCl$  and (B)  
 85  $Mg_2AlP$  using Gaussian line shapes.

86

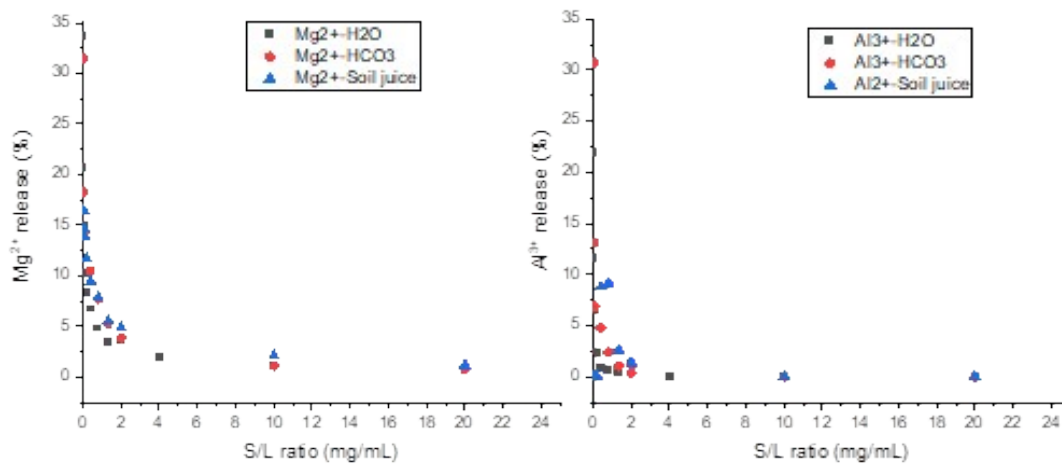
87

88



89

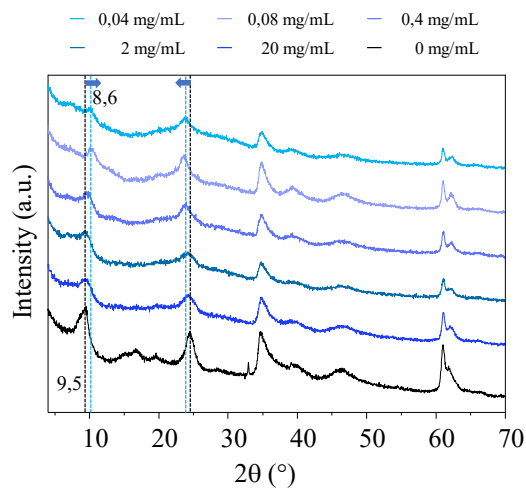
90 Figure S7. Kinetic of P release from  $Mg_2AlP$  at S/L at 20 mg/mL and 0.5 mg/mL (experimental data  
 91 points and fitted curves (dashed lines).



92

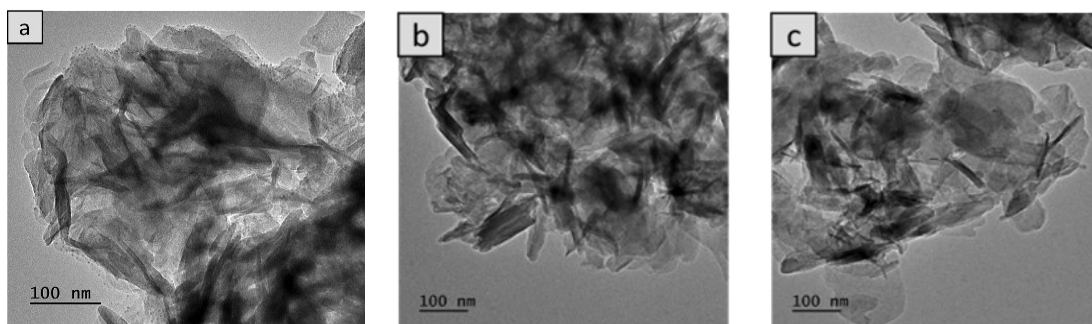
93 Figure S8.  $Mg^{2+}$  and  $Al^{3+}$  released (%) by  $Mg_2AlP$  at different S/L ratios in water,  $HCO_3^-$  solution  
 94 and soil juice.

95



96

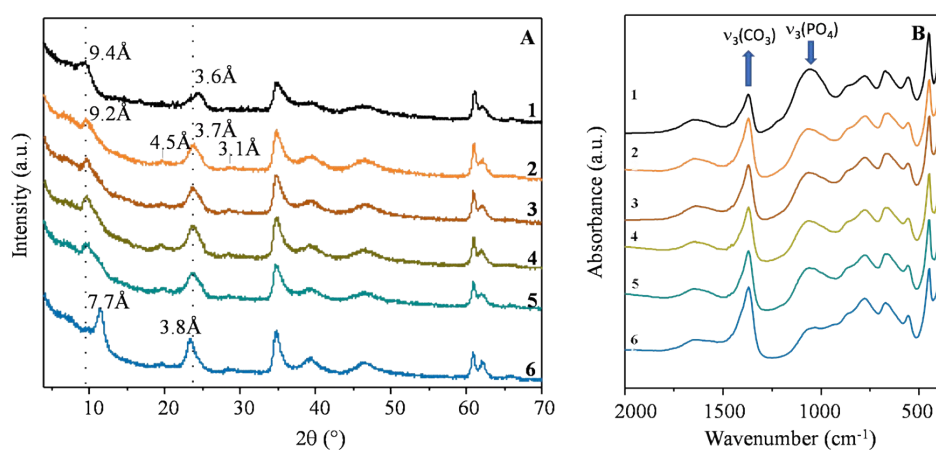
97 Figure S9. XRD of  $Mg_2AlP$  after 6 days release in  $H_2O$  at various S/L ratio.



98

99 Figure S10. TEM images of a)  $Mg_2AlP$  and residues after release in water at b) S/L 20 mg/mL and c)

100 S/L 0.04 mg/mL.



101

102 Figure S11. A) XRD patterns and B) FTIR spectra of  $Mg_2AlP$  (1) and solid residues after P release

103 trials (24h) at pH=4 (2), pH=6 (3), pH=8 (4), pH=10 (5), pH = 12 (6).

104



105 **Table**

106 Table S1: Phosphorus loading for 100% phosphate exchanged on Mg<sub>2</sub>Al(OH)<sub>6</sub>Cl.2H<sub>2</sub>O.

Phosphate species	PO <sub>4</sub> <sup>3-</sup>	HPO <sub>4</sub> <sup>2-</sup>	H <sub>2</sub> PO <sub>4</sub> <sup>-</sup>
P loading (mgP/gLDH)	22.6	33.9	67.8

107

108 Table S2: Release kinetic models.

Pseudo-second order model	Elovich model	Intraparticle diffusion model
$\frac{t}{Q_t} = \frac{1}{k_2 Q_e^2} + \frac{1}{Q_e} t$	$Q_t = 1/\beta \ln(\alpha\beta) + 1/\beta \ln t$	$Q_t = k \times t^{1/2} + L$
t : time Q <sub>t</sub> : [P] concentration at t Q <sub>e</sub> : equilibrium concentration, k <sub>2</sub> : reaction rate constant	α : initial rate (mg.g <sup>-1</sup> .min <sup>-1</sup> ) β : desorption constant as a function of release media, material surface and temperature	k : reaction rate constant L : limit layer thickness

109

110 Table S3: ICP-OES chemical composition of soil solution.

Chemical element	Na	K	Mg	Ca	Fe	Al	P	Zn	humic acid
Concentration (ppm)	>35	20	3.4	>35	-	0.0	0.5	0.0	~ 10

111

112